

# Time-Resolved 3D Quantitative Flow MRI of the Major Intracranial Arteries

R. Bammer<sup>1</sup>, T. Hope<sup>1</sup>, and M. T. Alley<sup>1</sup>

<sup>1</sup>Radiology, Stanford University, Stanford, CA, United States

**Introduction:** Exact knowledge of blood flow characteristics in cerebral vessels is of great relevance for diagnosing cerebro-vascular abnormalities since they are typically interlinked with abnormal flow to or within the neurocranium. To investigate the complex flow in major intracranial vessels we have recently developed a time-resolved, three-dimensional phase-contrast MRI method (4D-flow) in conjunction with advanced streamline processing and interactive visualization tools [1]. Despite its great merit 4D-flow applications are currently hindered by the substantial amount of data generated and measurement times involved. However, the high intravascular baseline-SNR renders 4D-flow an ideal candidate for use with parallel imaging. In addition, the extra SNR afforded by higher magnetic field strength provides the opportunity for even greater resolution. Therefore, the purpose of this study was to investigate the effect of field strength and parallel imaging on flow measurements when combined with 4D-flow. The success of this study would allow one to dramatically shorten scan time and/or resolve even more distal branches of the intracranial vascular system.

**Materials and Methods:** Eight healthy volunteers underwent head-to-head 4D-flow scanning on two whole-body MRI units (Signa LX) operating at 1.5T and 3.0T magnetic field strength. Both systems were equipped with high performance gradient systems (50 mT/m @ 1.5T, 40mT/m @ 3.0T, SR=150 mTs/m ea.). For MR signal reception a dedicated eight-channel head array coil (MRI Devices, Waukesha, WI) was used on both systems. At both scanners identical scanning parameters were used as follows: (180mm)<sup>2</sup> FOV, 90% rFOV, matrix = 300x180x30, TR/TE = 5.46ms/2.12ms, flip angle = 15°, NEX = 1, and RBW = 65kHz. For flow encoding, a  $v_{enc} = 100\text{cm/s}$  was chosen along each of the principal axes. Three section-direction phase encode steps per cardiac phase were selected to produce a high intrinsic temporal resolution of 65.5ms. For an HR of 70bpm a total of 1620 heart beats (NHB) were required leading to an overall acquisition time of 23.1min. A variant of GRAPPA [2] was used to speed-up image acquisition (24 ACS lines; kernel size =  $M_{kx} \times M_{ky} \times M_{coils} = 5 \times 4 \times 8$ ). The variable k-space sampling density led to net scan acceleration factors of 1.57 (13.3min) and 2.15 (10.0min) for ORFs of 2 and 3, respectively. Mean signal values obtained by ROI measurements served to extract velocity data from the left and right ICA and the basilar artery from each subject.

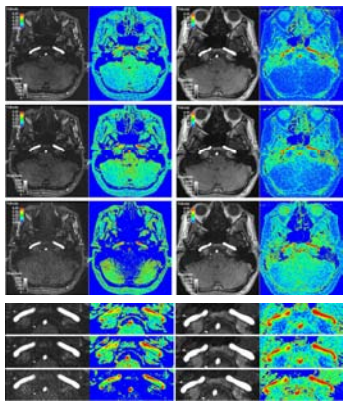


**Fig. 1 - Comparison of 4D flow imaging using different parallel imaging acceleration factors at 1.5T (column 1&2) and 3T (3&4). Top to bottom: ORFs of 1, 2, and 3. High velocities are encoded in red and yellow, whereas low velocities are encoded in green and blue. The 3T scans have substantially higher vessel contrast-to-noise ratio. For ORF=3 the parallel imaging related noise enhancement at 3T is comparable with that of ORF=2 at 1.5T. Both the magnitude image and speed image for ORF=3 at 1.5T demonstrates considerable noise enhancement (see zoomed up insert).**

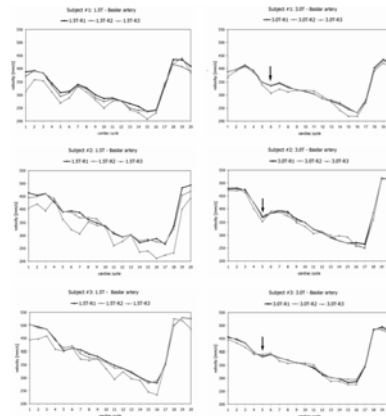


**Fig. 2 - The effect of parallel imaging acceleration (ORF=1 [bold black], ORF=2 [bold gray], and ORF=3 [thin gray]) on the measurement of velocities in the basilar artery over the cardiac cycle observed in three volunteers at 1.5T (left) and 3T (right). Each row shows the time course of velocity changes over the cardiac cycle in a different subject. Note that there are only little differences between the time course of ORF=1, 2, and 3 at 3T. Somewhat more significant deviations can be seen at 1.5T for ORF=2 and become substantial for ORF=3. In the presence of such significant fluctuations fine details in the time course, such as the dichrotic notch (arrow), are clearly missed.**

**Results:** Figure 1 shows a side-by-side comparison of 4D flow data using different ORFs for 1.5T and 3.0T at different GRAPPA accelerations. The increased baseline SNR is clearly apparent for the 3.0T data. It is also evident that at 1.5T the magnitude and velocity maps start to deteriorate when moving from two-fold to three-fold acceleration. Especially with an ORF=3 a significant SNR loss can be noticed in the mid-sagittal line (for example through the pons) due to the spatially varying SNR. The vessel baseline SNR for 1.5T ranged from 21-25 for the ICAs and 27-30 for the basilar artery. At 3T the corresponding SNR values ranged from 45-48 for the ICAs and 43-56 for the basilar artery. These measurements roughly represent the expected x2 SNR gain when moving from 1.5T to 3.0T. Depending on location, the SNR at 1.5T drops to 65%-68% and 24%-39% of its original value for ORF=2 and ORF=3, respectively, whereas at 3.0T the SNR drops only insignificantly to 91%-98% and 81%-89% of its original value for ORF=2 and ORF=3, respectively. Figure 2 shows the effect of GRAPPA on velocity time courses in three subjects for the basilar artery at 1.5T and 3.0T. The overall course of blood velocities can be seen at both field strengths and with all reduction factors. Only insignificant deviations are seen at 3.0T using different reduction factors. At 1.5T, the flow velocity measurements start to degrade with ORFs of 2 and clearly worsen with ORF=3. At 1.5T and with ORF=3 in all subjects blood velocity and flow through the basilar artery were underestimated throughout the entire cardiac cycle, and individual timepoints demonstrated greater fluctuations than with ORFs of 1 and 2. With an ORF=2 a slight increase in fluctuations was seen as well but no marked overall underestimation of flow was apparent. At 3T ORF=1 and ORF=2 measurements were practically identical and the ORF=3 scans had perturbations comparable to those at 1.5T with ORF between 1 and 2. Similar trends were observed for all other intracranial vessels (Table 1). Figure 3 shows example streamline visualizations [1] using ORF=2 at 3T.

**Table 1 - Blood velocity measurements at 1.5T and 3.0T: effect of GRAPPA**

	minimum velocity [mm/s]			maximum velocity [mm/s]			mean velocity [mm/s]			RMSE [mm/s]	
	X=1	X=2	X=3	X=1	X=2	X=3	X=1	X=2	X=3	X <sub>12</sub>	X <sub>13</sub>
1.5T	Basilar artery										
	230.1	248.6	258.7	454.3	440.6	434.2	333.1	340.1	339.7	17.1	23.8
	(±39.6)	(±37.0)	(±44.2)	(±59.2)	(±64.3)	(±69.2)	(±51.5)	(±50.6)	(±55.8)	(±3.22)	(±3.21)
Left ICA	216.5	219.6	232.0	428.3	414.1	401.6	293.0	307.7	307.5	18.1	28.4
	(±57.8)	(±59.2)	(±54.7)	(±116.5)	(±114.6)	(±117.1)	(±81.7)	(±82.0)	(±66.1)	(±3.37)	(±5.28)
	201.3	213.4	229.5	429.0	407.0	400.1	299.5	305.0	306.6	17.8	23.8
Right ICA	(±73.9)	(±76.3)	(±77.8)	(±141.9)	(±131.8)	(±134.3)	(±108.6)	(±103.0)	(±106.9)	(±3.22)	(±2.10)
3.0T	Basilar artery										
	243.1	252.8	262.9	462.9	437.9	431.2	346.9	345.3	343.0	18.7	26.1
	(±36.9)	(±37.1)	(±40.6)	(±48.4)	(±58.0)	(±49.1)	(±44.2)	(±53.7)	(±51.6)	(±5.47)	(±6.09)
Left ICA	216.4	226.5	236.5	446.5	409.8	403.2	315.7	313.7	313.1	15.6	28.1
	(±41.8)	(±43.6)	(±45.9)	(±90.6)	(±91.6)	(±95.0)	(±66.0)	(±64.2)	(±68.1)	(±2.34)	(±5.10)
	212.7	221.8	234.4	438.5	416.9	411.0	317.4	317.1	317.5	17.6	25.8
Right ICA	(±70.5)	(±74.0)	(±79.3)	(±125.0)	(±125.1)	(±129.2)	(±102.0)	(±103.6)	(±99.9)	(±4.03)	(±6.09)

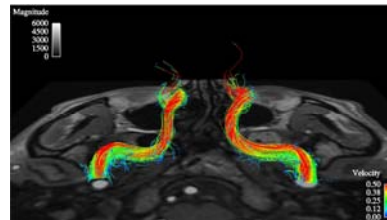


**Fig. 3 - Streamlines emanating from proximal seed regions in the ICA are visualized as they traverse the carotid canal towards the carotid siphon. The color of a streamline at a particular location reflects the measured local blood velocity. A helical flow pattern of the streamlines is well delineated as the blood flows distally through the carotid canal towards the siphon.**

at 3T without any significant flow errors, whereas at 1.5T the veracity of flow measurements using such high acceleration factors was consistently impaired. Therefore, at this field strength ORFs should not exceed two-fold acceleration factors. Certainly, these measurements have to be viewed in a relative perspective as the optimal choice of acceleration factors depends on scan parameters and several other factors such as FOV, type of array coil, slab orientation, and the fact that parallel imaging was applied only along one phase encode direction.

**References:** <sup>1</sup>Bammer R, et al. 13<sup>th</sup> ISMRM, Miami (FL), 2005, p. 530; <sup>2</sup>Griswold MA. 2nd Parallel Imaging WS, Zurich (CH), 2004;

**Acknowledgements:** This work was supported in part by the NIH (1R01EB002771), the Center of Advanced MR Technology at Stanford (P41RR09784), Lucas Foundation.